

$\{[1,4\text{-DHPyrazine}][\text{C}(\text{CN})_3]_2\}$ as a New Nano Molten Salt Catalyst for the Synthesis of Novel Piperazine Based bis(4-hydroxy-2H-chromen-2-one) Derivatives

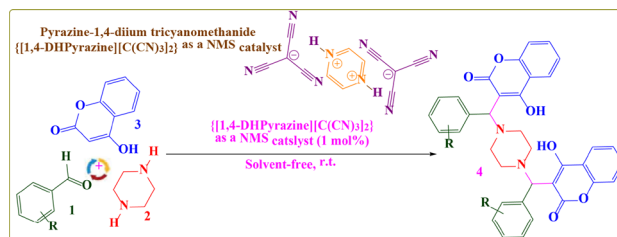
Saeed Baghery¹ · Mohammad Ali Zolfigol¹ · Romana Schirhagl² · Masoumeh Hasani^{2,3}

Received: 8 March 2017 / Accepted: 31 May 2017 / Published online: 12 June 2017
© Springer Science+Business Media, LLC 2017

Abstract In this article a convenient method for the synthesis of novel piperazine based bis(4-hydroxy-2H-chromen-2-one) derivatives using pyrazine-1,4-dium tricyanomethanide $\{[1,4\text{-DHPyrazine}][\text{C}(\text{CN})_3]_2\}$ as a new nanostructured molten salt (NMS) catalyst has been described. These compounds were synthesized via Mannich type reaction between several aromatic aldehyde, piperazine and 4-hydroxycoumarin under solvent-free condition at room temperature. The NMS catalyst was fully characterized via Fourier transform infrared (FT-IR), nuclear magnetic resonance (¹H NMR and ¹³C NMR), mass spectrometry, thermal gravimetric, derivative thermal gravimetric, differential thermal analysis, X-ray diffraction patterns, scanning electron microscopy and transmission electron microscopy analysis. The new compounds synthesized by using this NMS catalyst were also characterized by FT-IR, ¹H NMR and ¹³C NMR, high-resolution mass spectrometry techniques. The new NMS catalyst simply recovers and can be reused several times without significant loss of catalytic

activity. The major advantages of the described method in comparison to the classical reactions are low catalyst loading, short reaction time, high yields, simple isolation of product and reusability of the NMS catalyst.

Graphical Abstract Pyrazine-1,4-dium tricyanomethanide as a nano molten salt catalyst was designed, synthesized and used for the synthesis of novel biological piperazine based bis(4-hydroxy-2H-chromen-2-one) derivatives as bioactive and drug candidates.



Electronic supplementary material The online version of this article (doi:10.1007/s10562-017-2096-3) contains supplementary material, which is available to authorized users.

✉ Saeed Baghery
saadybaghery@yahoo.com

✉ Mohammad Ali Zolfigol
zolfi@basu.ac.ir; mzolfigol@yahoo.com

¹ Department of Organic Chemistry, Faculty of Chemistry, Bu-Ali Sina University, Hamedan 6517838683, Iran

² University Medical Center Groningen, Groningen University, Antonius Deusinglaan 1, 9713 AV Groningen, The Netherlands

³ Department of Analytical Chemistry, Faculty of Chemistry, Bu-Ali Sina University, Hamedan 6517838683, Iran

Keyword Pyrazine-1,4-dium tricyanomethanide $\{[1,4\text{-DHPyrazine}][\text{C}(\text{CN})_3]_2\}$ · 3,3'-(Piperazine-1,4-diylbis(arylmethylene))bis(4-hydroxy-2H-chromen-2-one) · Nanostructured molten salt (NMS)

1 Introduction

Among heterocyclic compounds, piperazine is a very important substrate in the pharmaceutical industry. Recently, attention has been drawn to considerable benefits of piperazine moieties for their versatile properties in pharmacology and chemistry [1–10]. Because of the derivatives' close link to numerous types of biological properties, for example anticancer [11], antiviral [12], anti-HIV [13], antibacterial [14], antifungal [15] and antimalarial [16],

piperazine moieties have been investigated widely by the organic chemists.

Molten salts (MSs) and ionic liquids (ILs) are both compounds solely composed of ions. MSs in the narrow concept are classified as high-temperature ILs but both definitions are often used interchangeably. The field of MSs and ILs has attracted an increasing amount of attention in the past decade generally because of their unique and tunable physicochemical properties and their flexibility in numerous uses [17–19]. As a unique class of solvents, MSs and ILs have many advantages including negligible vapor pressure, broad liquid ranges and excellent thermal stability. Furthermore, MSs and ILs are often described as ‘designer solvents’ since the combinations of cations and anions can be simply changed, and the resulting MSs and ILs can show preferred physicochemical and solvation properties [20–38].

In view of the need to the effective and eco-friendly chemicals and in continuation of our studies on the development of designing, synthesis and application of nanostructured molten salts (NMSs) and ionic liquids (NILs) as a multi-role materials, for extractive desulfurization [39], catalytic organic synthesis [40–42], nitration [43, 44], sulfonation [45], anomeric based oxidation [46–48] and etc., we have described a convenient method for the synthesis of piperazine based bis(4-hydroxy-2*H*-chromen-2-one)s under mild conditions (Scheme 1).

2 Experimental

2.1 General Information

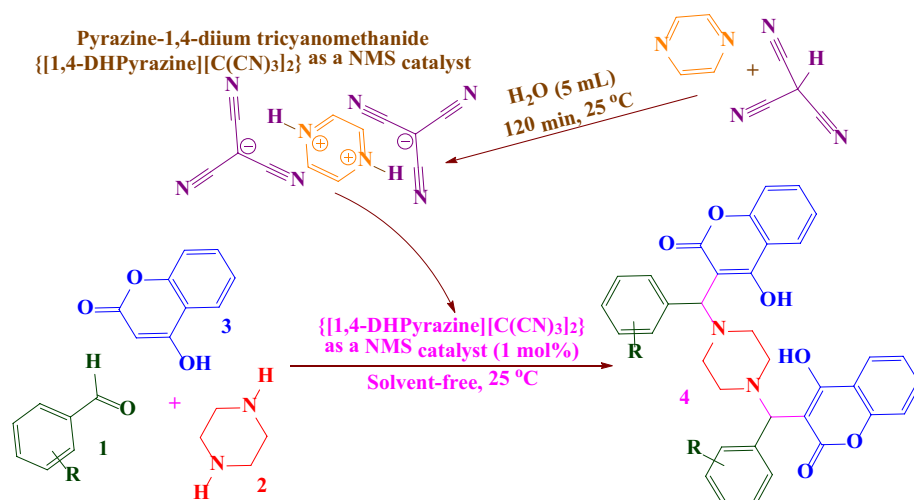
All chemicals and solvents were purchased from Merck, Fluka, Sigma-Aldrich and Across Organic Chemical Companies. All reagents were applied without any further

purification. Solvents were dried, distilled and stored over molecular sieves. The mass spectra were recorded on MS Model: 5975C VL MSD with Tripe-Axis Detector. ¹H NMR and ¹³C NMR spectra were attained using a Bruker DRX-400 spectrometer at 400 and 100 MHz, respectively by TMS as an internal standard in DMSO-*d*₆. TGA was performed with a Perkin–Elmer TGA at a heating rate of 10 °C min⁻¹ from room temperature to 600 °C. TLC was carried out on UV-active aluminium-backed silica gel plates F254. Melting points were measured with a thermo scientific apparatus and are uncorrected. FT-IR spectra were recorded with a Bruker spectrophotometer in KBr pellets. XRD patterns were recorded with a Bruker D8 ADVANCE diffractometer by Cu K_α radiation. SEM images were obtained with a KYKY-EM3200 and a maximum acceleration voltage of the primary electrons between 20 and 40 kV. TEM images were attained using a Zeiss-EM10C microscope with an accelerating voltage of 100 kV.

2.1.1 General Procedure for the Synthesis of Pyrazine-1,4-dium tricyanomethanide {[1,4-DHPyrazine][C(CN)₃]₂} as a Nanostructured Molten Salt Catalyst

To 5 mL of an aqueous solution of tricyanomethane (3 mmol; 0.273 g), pyrazine (3 mmol; 0.240 g) was added and the resulting mixture was stirred for 120 min at room temperature. Then the solvent was evaporated under reduced pressure. The white powder was dried under vacuum at 100 °C for 120 min. The achieved white solid was washed and filtered repeatedly with diethyl ether to remove any unreacted starting materials for attaining high purity, and then dried under vacuum. {[1,4-DHPyrazine][C(CN)₃]₂} was identified via FT-IR, ¹H NMR, ¹³C NMR, mass, TG, DTG, DTA, XRD, SEM and TEM analysis (Scheme 1).

Scheme 1 The synthesis of novel 3,3'-(piperazine-1,4-diylbis(arylmethylene)) bis(4-hydroxy-2*H*-chromen-2-one)s using pyrazine-1,4-dium tricyanomethanide {[1,4-DHPyrazine][C(CN)₃]₂} as a NMS catalyst



2.1.1.1 Pyrazine-1,4-dium tricyanomethanide {[1,4-DHPyrazine][C(CN)₃]₂} White solid; M.p.: >350 °C; Yield: 98% (0.771 g); IR (KBr): ν 3470, 2967, 2932, 2864, 2204, 2093, 1662, 1589, 1447, 1071 cm⁻¹; ¹H NMR (400 MHz, DMSO-*d*₆): δ_{ppm} 7.48 (s, 2H, ArH), 8.88 (s, 1H, —NH); ¹³C NMR (100 MHz, DMSO-*d*₆): δ_{ppm} 130.1, 142.0, 152.6; MS: m/z = 262.2 [M]⁺.

2.1.2 General Procedure for the Synthesis of 3,3'-(piperazine-1,4-diylbis(arylmethylene)) bis(4-hydroxy-2H-chromen-2-one) Derivatives

Pyrazine-1,4-dium tricyanomethanide {[1,4-DHPyrazine][C(CN)₃]₂} as a NMS catalyst (1 mol%; 0.0026 g) was added to a mixture of various aldehyde (1 mmol), 4-hydroxycoumarin (1 mmol; 0.162 g) and piperazine (1 mmol; 0.086 g) under solvent-free conditions at room temperature for an appropriate time. After completion of the reaction which was checked by TLC (*n*-hexane/ethyl acetate: 5/2), the resulting mixture was washed with water (10 mL) and filtered to separate catalyst from the other materials (the reaction mixture was insoluble in water and catalyst was soluble in water). The water was removed and the crude product was purified by recrystallization from ethanol/water (5:1) to yield pure products.

2.1.3 Spectral Data Analysis for Compounds

2.1.3.1 3,3'-(Piperazine-1,4-diylbis((4-chlorophenyl)methylene))bis(4-hydroxy-2H-chromen-2-one) (Table 4a, 5) White solid; M.p.: 253–255; Yield: 96%; IR (KBr): ν 3245, 3070, 2972, 2923, 1672, 1610, 1535, 1488, 1399, 1181 cm⁻¹; ¹H NMR (400 MHz, DMSO-*d*₆) δ_{ppm} 8.76 (s, 1H, —OH), 7.91 (d, J = 8.4 Hz, 0.5H, ArH), 7.81 (d, J = 7.7 Hz, 1H, ArH), 7.65 (d, J = 8.4 Hz, 0.5H, ArH), 7.49 (t, J = 7.7 Hz, 2H, ArH), 7.25 (d, J = 9.0 Hz, 1.5H, ArH), 7.20 (d, J = 9.4 Hz, 1.5H, ArH), 7.10 (d, J = 7.7 Hz, 1H, ArH), 6.24 (s, 1H, —CH aliphatic), 3.43 (s, 4H, —CH₂); ¹³C NMR (100 MHz, DMSO-*d*₆) δ_{ppm} 170.7, 167.6, 155.6, 144.3, 134.2, 132.4, 131.6, 130.7, 127.2, 126.1, 122.8, 118.6, 106.2, 38.8, 21.6; HRMS (ESI): m/z = 654.13244 [M]⁺.

2.1.3.2 3,3'-(Piperazine-1,4-diylbis((2,5-dimethoxyphenyl)methylene))bis(4-hydroxy-2H-chromen-2-one) (Table 4b, 5) White solid; M.p.: 244–246; Yield: 93%; IR (KBr): ν 3437, 3354, 3084, 2947, 1681, 1608, 1488, 1399, 1277 cm⁻¹; ¹H NMR (400 MHz, DMSO-*d*₆) δ_{ppm} 7.78 (d, J = 7.9 Hz, 1H, ArH), 7.44 (t, J = 7.7 Hz, 2H, ArH), 7.19 (d, J = 7.9 Hz, 2H, ArH), 7.16 (s, 1H, —OH), 6.77 (s, 1H, ArH), 6.69 (d, J = 8.7 Hz, 0.5H, ArH), 6.61 (d, J = 8.7 Hz, 0.5H, ArH), 6.16 (s, 1H, —CH aliphatic), 3.57 (s, 3H, —OCH₃), 3.44 (s, 3H, —OCH₃), 2.87 (s, 4H, —CH₂); ¹³C NMR

(100 MHz, DMSO-*d*₆) δ_{ppm} 170.2, 167.0, 155.6, 155.4, 154.7, 135.9, 133.6, 127.0, 125.8, 123.2, 119.8, 118.4, 114.9, 112.1, 106.6, 59.3, 58.1, 46.3, 35.9; HRMS (ESI): m/z = 706.25265 [M]⁺.

2.1.3.3 3,3'-(Piperazine-1,4-diylbis(phenylmethylene)) bis(4-hydroxy-2H-chromen-2-one) (Table 4c, 5) White solid; M.p.: 260–262; Yield: 91%; IR (KBr): ν 3445, 3010, 1681, 1634, 1612, 1562, 1402, 1199 cm⁻¹; ¹H NMR (400 MHz, DMSO-*d*₆) δ_{ppm} 8.50 (s, 1H, —OH), 7.79 (d, J = 7.6 Hz, 1H, ArH), 7.48 (t, J = 7.0 Hz, 2H, ArH), 7.24 (d, J = 8.7 Hz, 2H, ArH), 7.20 (d, J = 7.6 Hz, 1H, ArH), 7.14 (t, J = 7.6 Hz, 1H, ArH), 7.07 (t, J = 7.0 Hz, 2H, ArH), 6.25 (s, 1H, —CH aliphatic), 3.22 (s, 4H, —CH₂); ¹³C NMR (100 MHz, DMSO-*d*₆) δ_{ppm} 170.8, 167.7, 155.6, 145.4, 134.0, 130.7, 129.7, 127.9, 127.2, 125.9, 123.0, 118.5, 106.5, 43.7, 39.2; HRMS (ESI): m/z = 586.21039 [M]⁺.

2.1.3.4 3,3'-(Piperazine-1,4-diylbis(naphthalen-1-ylmethylene))bis(4-hydroxy-2H-chromen-2-one) (Table 4d, 5) Yellow solid; M.p.: 227–229; Yield: 96%; IR (KBr): ν 3442, 3049, 2955, 1668, 1605, 1527, 1397, 1032 cm⁻¹; ¹H NMR (400 MHz, DMSO-*d*₆) δ_{ppm} 8.00 (s, 1H, —OH), 7.80 (t, J = 7.6 Hz, 1H, ArH), 7.75 (d, J = 7.6 Hz, 1H, ArH), 7.66 (d, J = 8.1 Hz, 1H, ArH), 7.49 (d, J = 8.2 Hz, 1H, ArH), 7.45 (d, J = 8.3 Hz, 1H, ArH), 7.34 (t, J = 7.6 Hz, 2H, ArH), 7.23 (d, J = 8.2 Hz, 2H, ArH), 7.18 (t, J = 7.5 Hz, 2H, ArH), 6.72 (s, 1H, —CH aliphatic), 2.86 (s, 4H, —CH₂); ¹³C NMR (100 MHz, DMSO-*d*₆) δ_{ppm} 171.4, 167.2, 155.4, 141.6, 136.7, 134.7, 133.9, 131.5, 129.1, 128.8, 128.4, 128.0, 127.9, 127.3, 127.1, 126.0, 123.0, 118.5, 107.2, 46.4, 38.0; HRMS (ESI): m/z = 686.24169 [M]⁺.

2.1.3.5 3,3'-(Piperazine-1,4-diylbis((4-nitrophenyl)methylene))bis(4-hydroxy-2H-chromen-2-one) (Table 4e, 5) Cream solid; M.p.: 271–273; Yield: 98%; IR (KBr): ν 3443, 3082, 2909, 1676, 1603, 1516, 1406, 1347, 1181 cm⁻¹; ¹H NMR (400 MHz, DMSO-*d*₆) δ_{ppm} 8.05 (d, J = 7.8 Hz, 1H, ArH), 7.79 (d, J = 7.8 Hz, 1H, ArH), 7.51 (t, J = 7.7 Hz, 2H), 7.34 (d, J = 7.4 Hz, 1H, ArH), 7.27 (s, 1H, —OH), 7.25 (d, J = 5.1 Hz, 1H, ArH), 7.21 (d, J = 7.5 Hz, 2H, ArH), 6.33 (s, 1H, —CH aliphatic), 2.94 (s, 4H, —CH₂); ¹³C NMR (100 MHz, DMSO-*d*₆) δ_{ppm} 171.0, 167.4, 155.6, 154.6, 148.3, 134.3, 130.9, 127.2, 126.2, 126.1, 122.8, 118.6, 105.8, 45.7, 39.8; HRMS (ESI): m/z = 676.18054 [M]⁺.

2.1.3.6 3,3'-(piperazine-1,4-diylbis(2-methyl-3-phenylprop-2-ene-1,1-diyl))bis(4-hydroxy-2H-chromen-2-one) (Table 4f, 5) Cream solid; M.p.: 203–205; Yield: 91%; IR (KBr): ν 3446, 3058, 2968, 1709, 1634, 1601, 1514, 1414, 1107 cm⁻¹; ¹H NMR (400 MHz, DMSO-*d*₆) δ_{ppm} 7.83 (d, J = 8.0 Hz, 0.5H, ArH), 7.73 (d, J = 7.0 Hz, 0.5H, ArH),

7.63 (d, $J=8.8$ Hz, 0.5H, ArH), 7.57 (d, $J=8.6$ Hz, 0.5H, ArH), 7.46 (s, 1H, -OH), 7.36 (t, $J=7.0$ Hz, 1H, ArH), 7.29 (t, $J=7.6$ Hz, 2H, ArH), 7.20 (t, $J=7.0$ Hz, 2H, ArH), 7.12 (d, $J=8.0$ Hz, 1H, ArH), 7.03 (d, $J=7.5$ Hz, 0.5H, ArH), 7.00 (d, $J=7.8$ Hz, 0.5H, ArH), 6.30 (s, 1H, -CH aliphatic), 3.75 (s, 1H, -CH), 2.81 (s, 4H, -CH₂), 1.34 (s, 3H, -CH₃); ¹³C NMR (100 MHz, DMSO-d₆) δ_{ppm} 162.5, 156.6, 155.6, 155.3, 135.3, 132.1, 131.8, 131.0, 130.9, 130.6, 127.7, 125.8, 125.2, 119.5, 118.5, 118.2, 115.6, 47.0, 22.3, 17.6; HRMS (ESI): $m/z=666.27299$ [M]⁺.

2.1.3.7 3,3'-(Piperazine-1,4-diylbis((3-nitrophenyl)methylene))bis(4-hydroxy-2H-chromen-2-one) (Table 4g, 5) Cream solid; M.p.: 238–240; Yield: 96%; IR (KBr): ν 3451, 3070, 1678, 1607, 1528, 1398, 1348, 1276, 1107 cm⁻¹; ¹H NMR (400 MHz, DMSO-d₆) δ_{ppm} 7.97 (d, $J=8.0$ Hz, 0.5H, ArH), 7.87 (s, 1H, -OH), 7.80 (d, $J=7.8$ Hz, 1H, ArH), 7.55 (t, $J=7.6$ Hz, 1H, ArH), 7.50 (d, $J=7.0$ Hz, 1H, ArH, ArH), 7.46 (d, $J=7.9$ Hz, 0.5H, ArH), 7.27 (d, $J=8.2$ Hz, 1H, ArH), 7.22 (t, $J=7.5$ Hz, 2H, ArH), 6.34 (s, 1H, ArH), 5.73 (s, 1H, -CH aliphatic), 2.87 (s, 4H, -CH₂); ¹³C NMR (100 MHz, DMSO-d₆) δ_{ppm} 171.0, 167.4, 155.6, 150.8, 148.2, 136.9, 134.3, 132.4, 127.2, 126.1, 124.1, 123.4, 122.7, 118.7, 105.7, 46.2, 39.3; HRMS (ESI): $m/z=676.18054$ [M]⁺.

2.1.3.8 3,3'-(Piperazine-1,4-diylbis((4-hydroxyphenyl)methylene))bis(4-hydroxy-2H-chromen-2-one) (Table 4h, 5) Yellow solid; M.p.: 215–217; Yield: 92%; IR (KBr): ν 3273, 3164, 3035, 2969, 1678, 1638, 1607, 1514, 1399, 1054 cm⁻¹; ¹H NMR (400 MHz, DMSO-d₆) δ_{ppm} 8.90 (s, 1H, -OH), 7.79 (d, $J=7.6$ Hz, 1H, ArH), 7.47 (t, $J=7.4$ Hz, 2H, ArH), 7.22 (d, $J=7.9$ Hz, 2H, ArH), 7.19 (d, $J=7.6$ Hz, 1H, ArH), 6.86 (d, $J=7.3$ Hz, 1H, ArH), 6.53 (d, $J=6.1$ Hz, 1H, ArH), 6.14 (s, 1H, -CH aliphatic), 4.33 (s, 1H, -OH), 2.90 (s, 4H, -CH₂); ¹³C NMR (100 MHz, DMSO-d₆) δ_{ppm} 170.6, 167.6, 157.7, 155.5, 135.3, 133.8, 130.6, 127.1, 125.9, 123.1, 118.5, 117.5, 106.9, 46.0, 38.4; HRMS (ESI): $m/z=618.20022$ [M]⁺.

2.1.3.9 3,3'-(Piperazine-1,4-diylbis((4-(dimethylamino)phenyl)methylene))bis(4-hydroxy-2H-chromen-2-one) (Table 4i, 5) Pink solid; M.p.: 233–235; Yield: 93%; IR (KBr): ν 3425, 3167, 2968, 1677, 1631, 1610, 1513, 1391, 1181 cm⁻¹; ¹H NMR (400 MHz, DMSO-d₆) δ_{ppm} 7.79 (d, $J=7.8$ Hz, 2H, ArH), 7.47 (t, $J=7.0$ Hz, 1H, ArH), 7.21 (t, $J=7.6$ Hz, 1H, ArH), 7.18 (s, 1H, -OH), 6.88 (d, $J=8.4$ Hz, 2H, ArH), 6.54 (d, $J=8.7$ Hz, 2H, ArH), 6.15 (s, 1H, -CH aliphatic), 2.93 (s, 4H, -CH₂), 2.48 (s, 6H, -CH₃); ¹³C NMR (100 MHz, DMSO-d₆) δ_{ppm} 170.6, 167.7, 155.5, 151.3, 133.8, 133.2, 130.3, 127.1, 125.8, 123.1, 118.4, 115.5, 106.9, 45.7, 43.6, 38.2; HRMS (ESI): $m/z=672.29479$ [M]⁺.

2.1.3.10 3,3'-(Piperazine-1,4-diylbis(furan-2-ylmethylene))bis(4-hydroxy-2H-chromen-2-one) (Table 4j, 5) Brown solid; M.p.: 324–326; Yield: 90%; IR (KBr): ν 3437, 3064, 1674, 1605, 1519, 1415, 1212 cm⁻¹; ¹H NMR (400 MHz, DMSO-d₆) δ_{ppm} 7.79–7.85 (s, 1H, -OH), 7.81 (d, $J=7.9$ Hz, 1H, ArH), 7.48 (t, $J=7.6$ Hz, 1H, ArH), 7.33 (d, $J=7.7$ Hz, 1H, ArH), 7.21 (t, $J=7.6$ Hz, 2H, ArH), 7.15 (d, $J=8.9$ Hz, 1H, ArH), 7.10 (d, $J=8.0$ Hz, 1H, ArH), 5.87 (s, 1H, -CH aliphatic), 3.05 (s, 4H, -CH₂); ¹³C NMR (100 MHz, DMSO-d₆) δ_{ppm} 181.0, 158.1, 155.5, 150.1, 143.6, 136.2, 134.0, 130.9, 127.2, 126.0, 118.5, 112.9, 107.8, 34.1, 21.4; HRMS (ESI): $m/z=566.16892$ [M]⁺.

2.1.3.11 3,3'-(Piperazine-1,4-diylbis(thiophen-2-ylmethylene))bis(4-hydroxy-2H-chromen-2-one) (Table 4k, 5) Brown solid; M.p.: 242–244; Yield: 90%; IR (KBr): ν 3445, 3094, 2923, 1673, 1608, 1557, 1400, 1183 cm⁻¹; ¹H NMR (400 MHz, DMSO-d₆) δ_{ppm} 7.82 (d, $J=7.8$ Hz, 1H, ArH), 7.49 (t, $J=7.7$ Hz, 2H, ArH), 7.24 (d, $J=3.3$ Hz, 1H, ArH), 7.21 (d, $J=7.6$ Hz, 1H, ArH), 7.11 (d, $J=5.0$ Hz, 1H, ArH), 6.77 (t, $J=7.6$ Hz, 1H, ArH), 6.56 (s, 1H, -OH), 6.39 (s, 1H, -CH aliphatic), 2.89 (s, 4H, -CH₂); ¹³C NMR (100 MHz, DMSO-d₆) δ_{ppm} 170.9, 167.1, 155.5, 151.2, 134.1, 129.2, 127.3, 126.1, 126.0, 125.7, 122.9, 118.5, 106.8, 46.13, 36.0; HRMS (ESI): $m/z=598.12323$ [M]⁺.

2.1.3.12 3,3'-(Piperazine-1,4-diylbis((3-hydroxyphenyl)methylene))bis(4-hydroxy-2H-chromen-2-one) (Table 4l, 5) Yellow solid; M.p.: 221–223; Yield: 90%; IR (KBr): ν 3379, 3069, 2963, 1663, 1610, 1559, 1534, 1401, 1107 cm⁻¹; ¹H NMR (400 MHz, DMSO-d₆) δ_{ppm} 8.88 (s, 1H, -OH), 7.80 (d, $J=7.7$ Hz, 1H, ArH), 7.48 (t, $J=8.3$ Hz, 2H, ArH), 7.34 (s, 1H, -OH), 7.23 (d, $J=7.9$ Hz, 1H, ArH), 7.19 (d, $J=7.5$ Hz, 1H, ArH), 6.90 (t, $J=7.8$ Hz, 1H, ArH), 6.54 (s, 1H, ArH), 6.49 (d, $J=7.8$ Hz, 0.5H, ArH), 6.43 (d, $J=7.9$ Hz, 0.5H, ArH), 6.16 (s, 1H, -CH aliphatic), 2.87 (s, 4H, -CH₂); ¹³C NMR (100 MHz, DMSO-d₆) δ_{ppm} 170.7, 167.6, 160.0, 155.6, 147.0, 133.9, 131.5, 127.2, 125.9, 123.1, 120.5, 118.5, 116.8, 114.9, 106.5, 46.2, 39.1; HRMS (ESI): $m/z=618.20022$ [M]⁺.

2.1.3.13 3,3'-(Piperazine-1,4-diylbis(pyridin-4-ylmethylene))bis(4-hydroxy-2H-chromen-2-one) (Table 4 m, 5) Yellow solid; M.p.: 254–256; Yield: 90%; IR (KBr): ν 3419, 3069, 2957, 1673, 1605, 1540, 1452, 1411, 1182 cm⁻¹; ¹H NMR (400 MHz, DMSO-d₆) δ_{ppm} 8.31 (d, $J=5.8$ Hz, 2H, ArH), 7.79 (d, $J=7.0$ Hz, 2H, ArH), 7.50 (t, $J=7.3$ Hz, 1H, ArH), 7.25 (t, $J=7.6$ Hz, 1H, ArH), 7.20 (s, 1H, -OH), 7.11 (d, $J=4.4$ Hz, 2H, ArH), 6.25 (s, 1H, -CH aliphatic), 2.87 (s, 4H, -CH₂); ¹³C NMR (100 MHz, DMSO-d₆) δ_{ppm} 170.9, 167.4, 155.6, 151.9, 134.3, 131.2, 127.2, 126.1, 125.5, 122.7, 118.6, 105.2, 46.2, 39.2; MS: $m/z=588.20$ [M]⁺.

2.1.3.14 3,3'-(Piperazine-1,4-diylbis((2,4-dichlorophenyl)methylene))bis(4-hydroxy-2H-chromen-2-one) (Table 4n, 5) Cream solid; M.p.: 218–220; Yield: 95%; IR (KBr): ν 3434, 3064, 2960, 1672, 1606, 1532, 1466, 1400, 1329, 1182 cm^{-1} ; ¹H NMR (400 MHz, DMSO-d₆) δ_{ppm} 7.79 (d, $J=7.5$ Hz, 1H, ArH), 7.48 (t, $J=7.3$ Hz, 3H, ArH), 7.39 (s, 1H, ArH), 7.36 (s, 1H, -OH), 7.26 (d, $J=13.0$ Hz, 2H, ArH), 7.20 (d, $J=8.1$ Hz, 1H, ArH), 6.10 (s, 1H, -CH aliphatic), 2.88 (s, 4H, -CH₂); ¹³C NMR (100 MHz, DMSO-d₆) δ_{ppm} 170.8, 166.8, 155.5, 142.7, 136.5, 134.7, 134.0, 133.6, 131.7, 129.2, 127.1, 126.0, 122.8, 118.5, 105.4, 46.2, 38.9; MS: $m/z=722.05$ [M]⁺.

2.1.3.15 3,3'-(Piperazine-1,4-diylbis((3,4-dimethoxyphenyl)methylene))bis(4-hydroxy-2H-chromen-2-one) (Table 4o, 5) White solid; M.p.: 269–271; Yield: 93%; IR (KBr): ν 3133, 3032, 2957, 1674, 1654, 1623, 1513, 1182 cm^{-1} ; ¹H NMR (400 MHz, DMSO-d₆) δ_{ppm} 7.80 (d, $J=7.6$ Hz, 1H, ArH), 7.47 (t, $J=7.6$ Hz, 2H, ArH), 7.24 (d, $J=4.4$ Hz, 1H, ArH), 7.21 (d, $J=3.7$ Hz, 1H, ArH), 7.18 (s, 1H, ArH), 6.74 (d, $J=8.3$ Hz, 0.5H, ArH), 6.64 (d, $J=4.2$ Hz, 0.5H, ArH), 6.60 (s, 1H, -CH aliphatic), 3.66 (s, 3H, -OCH₃), 3.50 (s, 3H, -OCH₃), 2.95 (s, 4H, -CH₂); ¹³C NMR (100 MHz, DMSO-d₆) δ_{ppm} 170.7, 167.6, 155.5, 151.3, 149.6, 138.0, 133.9, 127.1, 125.9, 123.0, 122.0, 118.5, 114.6, 114.5, 106.7, 58.6, 58.5, 46.0, 38.8; MS: $m/z=706.25$ [M]⁺.

3 Results and Discussion

In this paper, we designed and synthesized a good range of novel 3,3'-(piperazine-1,4-diylbis(arylmethylene))bis(4-hydroxy-2H-chromen-2-one)s via condensation reaction

between piperazine, 4-hydroxycoumarin and various aldehydes in the presence of pyrazine-1,4-dium tricyanomethanide {[1,4-DHPyrazine][C(CN)₃]₂} as a new nanostructured molten salt (NMS) catalyst under solvent-free conditions at room temperature (Scheme 1).

3.1 Characterization of Pyrazine-1,4-dium tricyanomethanide {[1,4-DHPyrazine][C(CN)₃]₂} as a Nanostructured Molten Salt Catalyst

The structure of {[1,4-DHPyrazine][C(CN)₃]₂} as a NMS catalyst was studied and fully characterized by FT-IR, ¹H NMR, ¹³C NMR, mass, TG, DTG, DTA, XRD, SEM and TEM analysis.

In the FT-IR spectrum of the new NMS catalyst, {[1,4-DHPyrazine][C(CN)₃]₂}, the absorption band at 1662 cm^{-1} is linked to vibrational modes of C=N bonds of tricyanomethanide counter ion. Moreover, the identified peak at 2204 and 2093 cm^{-1} related to C≡N stretching group on tricyanomethanide counter ion. Also, the known peak at 3470 cm^{-1} is assigned to N-H stretching of pyrazine-1,4-dium. The changes in FT-IR spectrum of {[1,4-DHPyrazine][C(CN)₃]₂} in comparison with tricyanomethane and pyrazine is a confirmation of production of NMS catalyst (Fig. 1).

The ¹H NMR spectrum of the catalyst {[1,4-DHPyrazine][C(CN)₃]₂} shows two singlet peaks at 7.48 and 8.88 ppm that can be assigned to the aromatic ring protons of pyrazine-1,4-dium and N-H group on pyrazine-1,4-dium, respectively (Fig. 2).

Presence of three signals in the ¹³C NMR spectrum are also in agreement with the structure of {[1,4-DHPyrazine][C(CN)₃]₂} catalyst. The important peaks of ¹³C NMR spectrum of the NMS catalyst are the peak at $\delta=152.6$

Fig. 1 The FT-IR spectrum of a tricyanomethane; b pyrazine; c {[1,4-DHPyrazine][C(CN)₃]₂} as a NMS catalyst

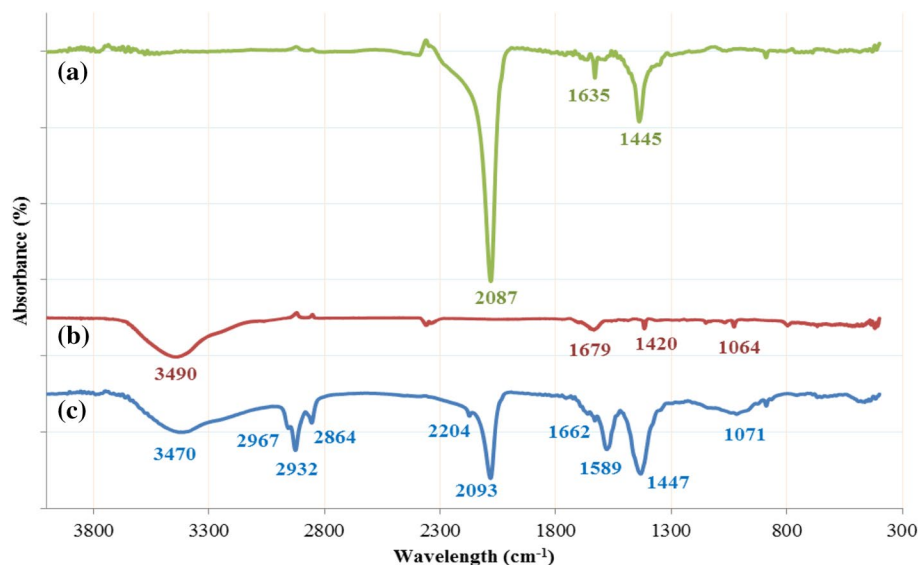
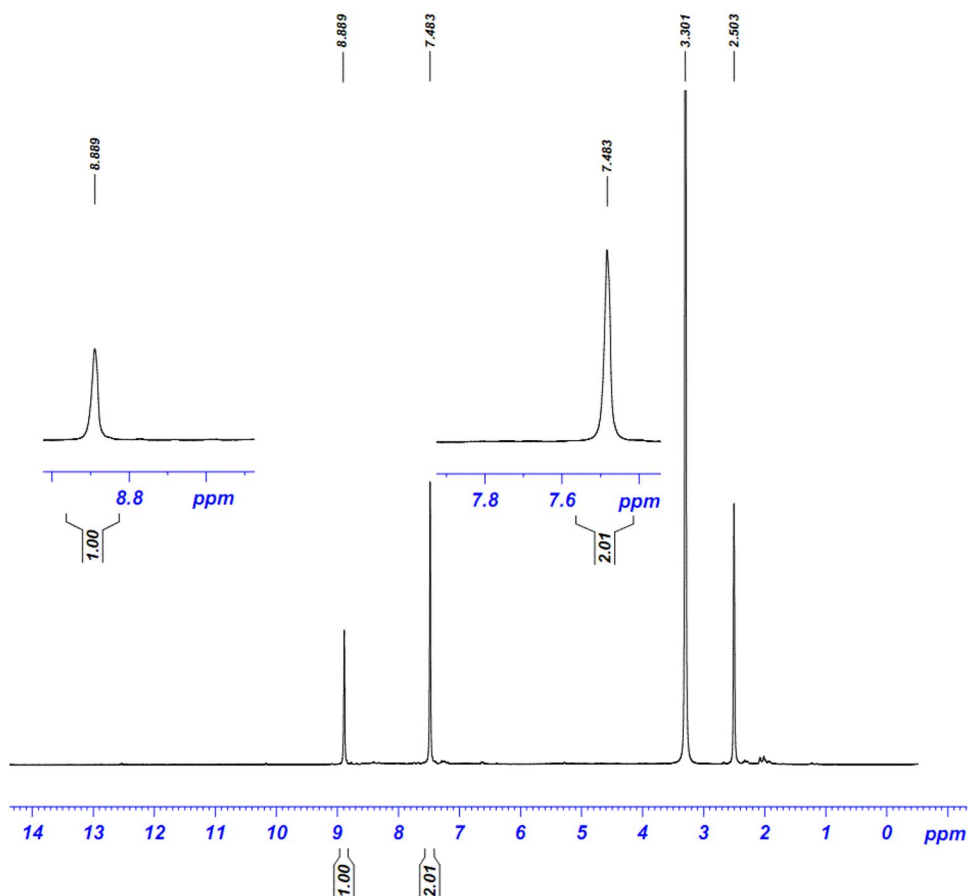


Fig. 2 The ^1H NMR spectrum of the NMS catalyst $\{[1,4\text{-DHPyrazine}][\text{C}(\text{CN})_3]_2\}$



which is related to the $\text{C}\equiv\text{N}$ group of tricyanomethanide counter ion and the peak at $\delta = 130.1$ ppm that is assigned to the carbon connected to the three cyanide groups ($-\text{C}(\text{CN})_3$). Furthermore, the known peak at 142.0 ppm is related to aromatic ring carbons of pyrazine-1,4-dium (Fig. 3). From all the changes in the carbon and proton NMR chemical shifts, the conclusion can be drawn that the new NMS catalyst has been successfully prepared (Figs. S1 and S2).

The mass spectrum (EI, 70 eV) of $\{[1,4\text{-DHPyrazine}][\text{C}(\text{CN})_3]_2\}$ catalyst was in good agreement with what we expected. The molecular ion peak (M^+) was detected at $m/z = 262.2$ which is equivalent to the catalyst molecular weight. Additionally, the peaks at $m/z = 90.0$ and $m/z = 82.1$ corresponded to the tricyanomethanide and pyrazine-1,4-dium fragments, respectively (Fig. 4).

Figures 5 and 6 display the thermal behaviour of our new NMS catalyst. Thermal analysis (TGA/DTG/DTA) of the $\{[1,4\text{-DHPyrazine}][\text{C}(\text{CN})_3]_2\}$ shows two peaks (The DTA analysis diagram is downward because of the exothermic decomposition of NMS catalyst) between room temperature and 450°C . The mechanism proposed in the thermal decomposition involves the breakdown of the compound in the range of 190 to 305°C and the subsequent

removal of the surface-adsorbed solvent and counter ion. The initial weight loss is about 45%. The second weight loss region between 360 and 450°C is attributed to the continuing decomposition of organic compound. The weight loss in this step is about 55%. No higher weight loss was observed at higher temperatures.

The size, shape and morphology of $\{[1,4\text{-DHPyrazine}][\text{C}(\text{CN})_3]_2\}$ were characterized using XRD pattern, SEM and TEM analysis. X-ray diffraction pattern of $\{[1,4\text{-DHPyrazine}][\text{C}(\text{CN})_3]_2\}$ was obtained in solid state form (Fig. 7). The eight XRD characteristic peaks at 23.60° , 27.30° , 30.70° , 31.70° , 39.00° , 46.10° , 63.70° and 75.60° , indicate the crystallographic planes of the NMS catalyst, can be obviously detected. The corresponding XRD data are given in Table 1. Usually, solid materials are classified as being either crystalline or amorphous. In crystalline materials the ions occupy specific locations in a regular lattice. The results of investigations of XRD analysis display the NMS catalyst as nanometer-sized crystallites. The average crystallite diameter was calculated via the Scherrer equation [$D = K\lambda/(\beta \cos\theta)$] by the peak broadening (FWHM) of the most intense diffraction peak (27.30°). The SEM and TEM images in Fig. 8 show that the NMS particles

Fig. 3 The ¹³C NMR spectrum of the NMS catalyst {[1,4-DHPyrazine][C(CN)₃]₂}

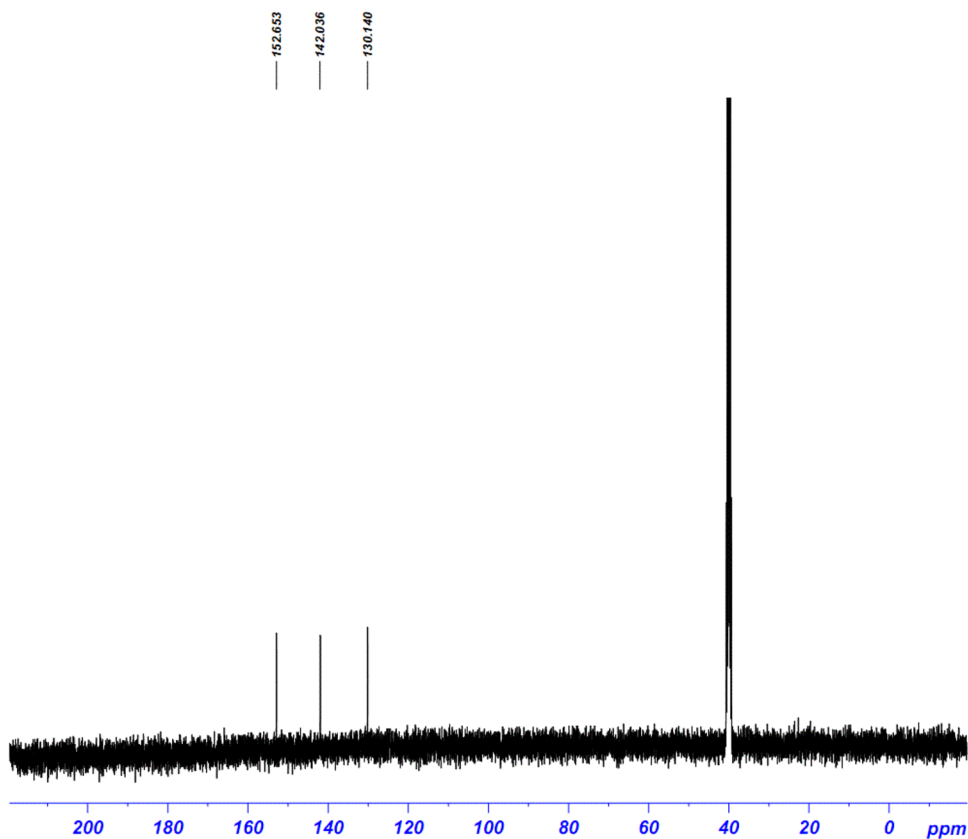
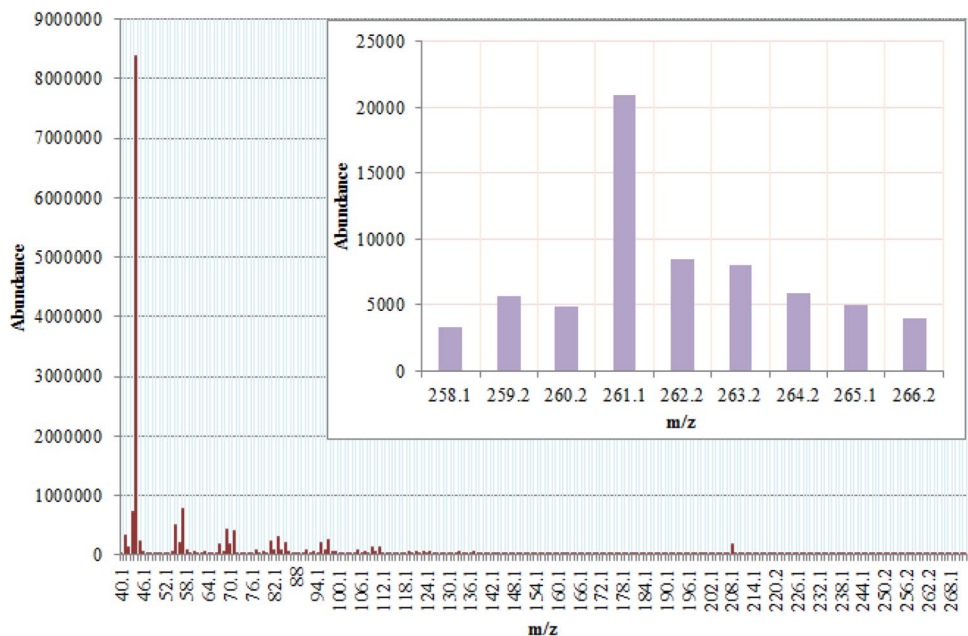


Fig. 4 The mass spectrum of the NMS catalyst {[1,4-DHPyrazine][C(CN)₃]₂}



have a rather spherical morphology with good monodispersity. It can be noted that a fair uniform dispersion of small particles around 25–72 nm of NMS catalyst has been obtained through our synthesis method. An average

crystallite size of 12.78 nm can be reported according to XRD pattern, SEM and TEM images and histogram of TEM analysis.

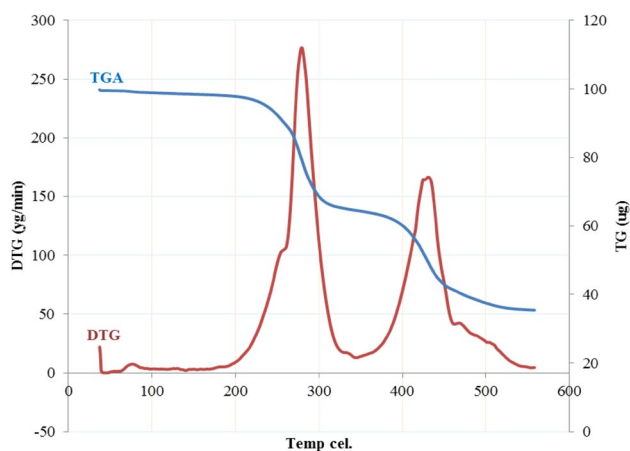


Fig. 5 The thermal gravimetric analysis (TGA) and derivative thermal gravimetric analysis (DTG) of the NMS catalyst {[1,4-DHPyrazine][C(CN)₃]₂}

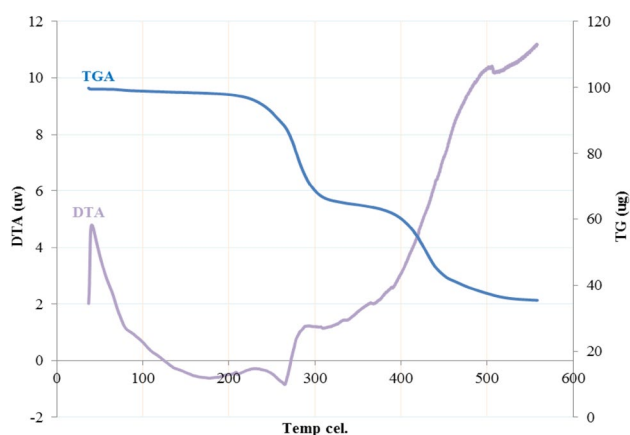
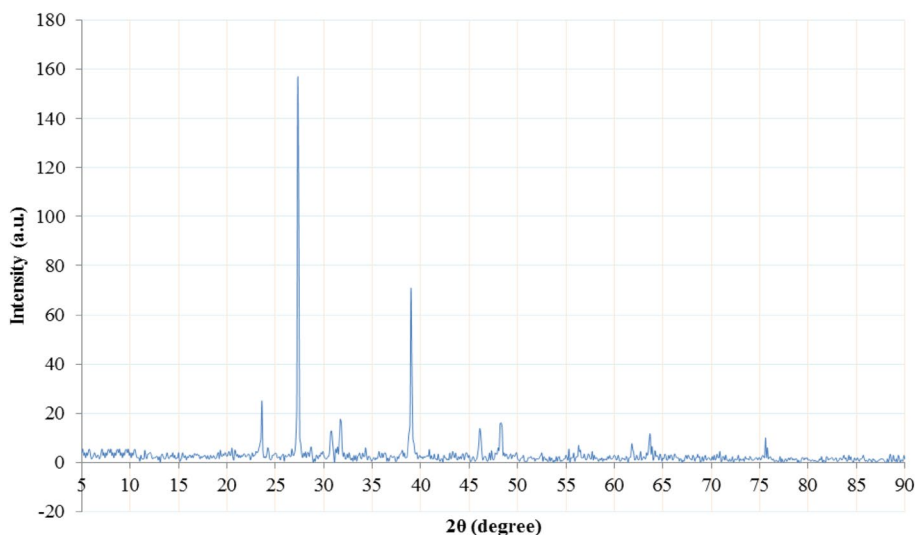


Fig. 6 The thermal gravimetric analysis (TGA) and differential thermal analysis (DTA) of the NMS catalyst {[1,4-DHPyrazine][C(CN)₃]₂}

Fig. 7 The XRD pattern of the NMS catalyst {[1,4-DHPyrazine][C(CN)₃]₂}



3.2 Application of {[1,4-DHPyrazine][C(CN)₃]₂} Catalyst in the Synthesis of 3,3'-(piperazine-1,4-diylbis(arylmethylene))bis(4-hydroxy-2H-chromen-2-one) Derivatives

In order to investigate the catalytic activity of {[1,4-DHPyrazine][C(CN)₃]₂}, the condensation reaction of 4-chlorobenzaldehyde, 4-hydroxycoumarin and piperazine as a model reaction was performed under solvent-free condition using different amounts of various catalysts (Table 2). As is obvious by the results, {[1,4-DHPyrazine][C(CN)₃]₂} is the most efficient catalyst in terms of yield of product, while the other catalysts lead to product with yields of 60–90%.

In order to optimize the reaction condition, different experimental parameters were tested, for the model reaction in the presence of various amount of the new NMS catalyst. The amount of the catalyst and temperature were optimized under solvent-free conditions. As seen from Tables 3 and 1 mol% (0.0026 g) of NMS was found to be the optimum amount of the catalyst (Table 3, entries 7 and 8). There was no significant change in the yield of products when larger amounts of NMS catalyst were applied (Table 3, entries 10–12). The effect of temperature was also investigated by performing the model reaction at various temperatures (room temperature, 50 and 100 °C) while the amount of NMS catalyst has been kept constant. The best result is achieved at room temperature (Table 3, entry 7). It is worth mentioning that under catalyst-free condition, such a synthesis was not possible (Table 3, entries 1–3).

To display the applicability of the synthesized NMS catalyst in different organic reactions, {[1,4-DHPyrazine][C(CN)₃]₂} was applied to the synthesis of 3,3'-(piperazine-1,4-diylbis(arylmethylene))bis(4-hydroxy-2H-chromen-2-one) derivatives at room temperature. Again the reaction

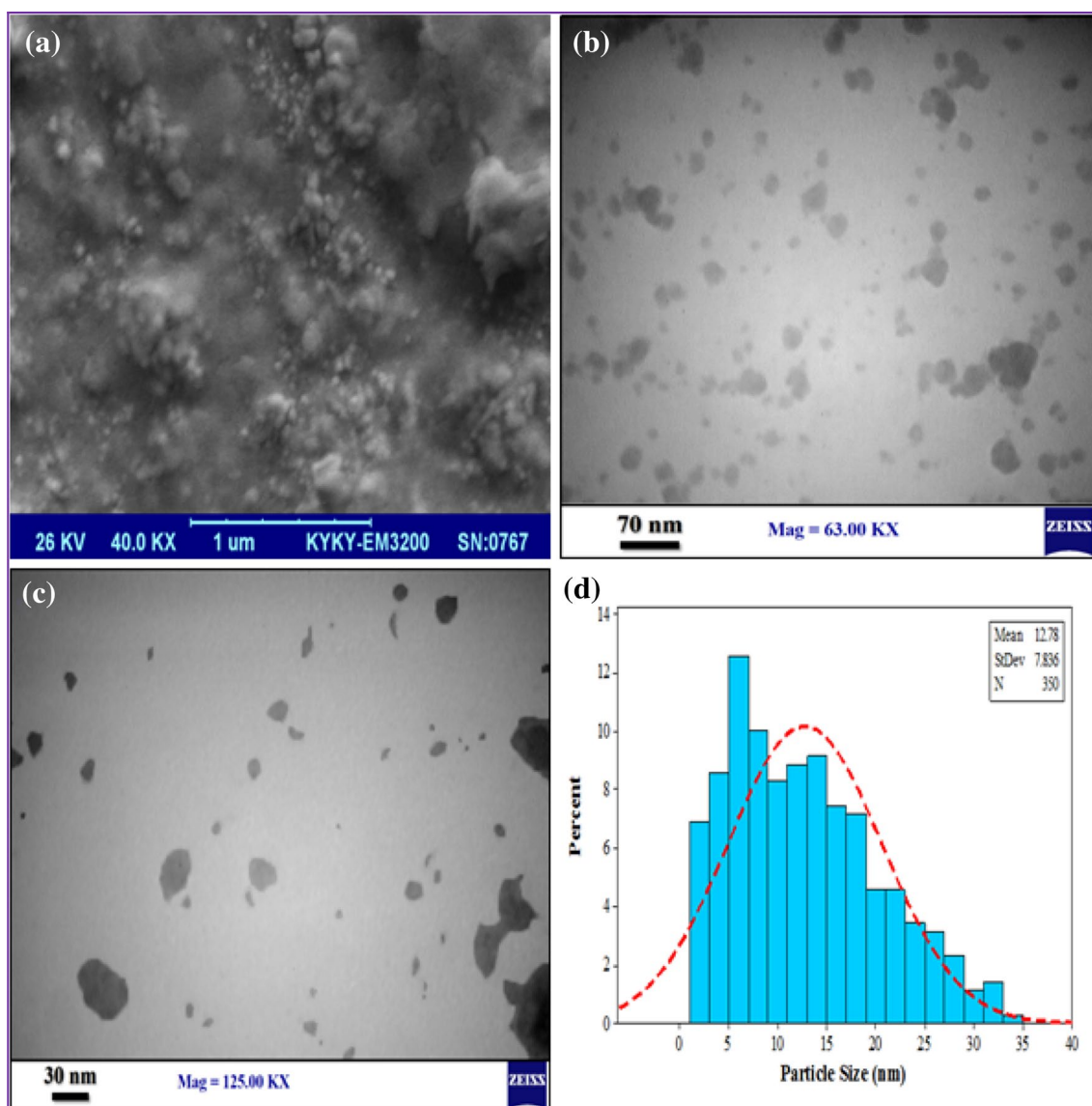


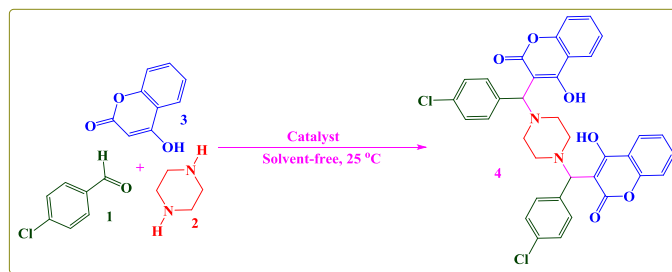
Fig. 8 The SEM (a), TEM (b and c) and histogram of TEM analysis (d) of the NMS catalyst {[1,4-DHPyrazine][C(CN)₃]₂}

Table 1 X-ray diffraction (XRD) data for the NMS catalyst {[1,4-DHPyrazine][C(CN)₃]₂}

Entry	2θ	Peak width [FWHM] (degree)	Size [nm]	Inter planer distance [nm]
1	23.60	0.14	57.98	0.376735
2	27.30	0.18	45.42	0.326285
3	30.70	0.32	25.75	0.290879
4	31.70	0.31	26.64	0.281927
5	39.00	0.17	49.57	0.230672
6	46.10	0.30	28.78	0.196662
7	63.70	0.23	40.67	0.145917
8	75.60	0.14	71.83	0.125631

between 4-chlorobenzaldehyde, 4-hydroxycoumarin and piperazine was chosen as a model, and this model reaction was examined in common organic solvents with varying polarities (Table 4). We found that the reaction proceeded readily in polar solvents (Table 4, entries 2 and 3), but the product yields decreased by decreasing the solvent polarities (Table 4, entries 5–8). The results show that the best efficacy and the highest yield are attained under solvent-free conditions as a green approach (Table 4, entry 1).

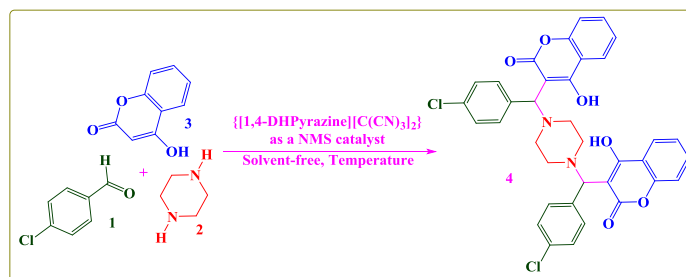
To study the efficacy and applicability of this NMS catalyst in the synthesis of 3,3'-(piperazine-1,4-diylbis(arylmethylene))bis(4-hydroxy-2H-chromen-2-one) derivatives, the reaction was extended to other substituted aldehydes at room temperature under solvent-free condition. The results are summarized in Table 5. In

Table 2 Reaction between 4-chlorobenzaldehyde, 4-hydroxycoumarin and piperazine in the presence of various catalytic systems

Entry	Catalyst	Catalyst loading (mol%)	Time (min)	Yield ^a (%)
1	{[1,4-DHPyrazine][C(CN) ₃] ₂ }	1	5	96
2	[Msim]Cl	2	15	90
3	[Dsim]Cl	2	15	87
4	CAN	5	30	81
5	Acetic acid	10	30	75
6	H ₃ PW ₁₂ O ₄₀	5	30	85
7	NH ₂ SO ₃ H	10	60	65
8	Ce(HSO ₄) ₃ ·7H ₂ O	10	60	60

Reaction condition: 4-Chlorobenzaldehyde (1 mmol; 0.140 g), 4-hydroxycoumarin (1 mmol; 0.162 g), piperazine (1 mmol; 0.086 g)

^aIsolated yield

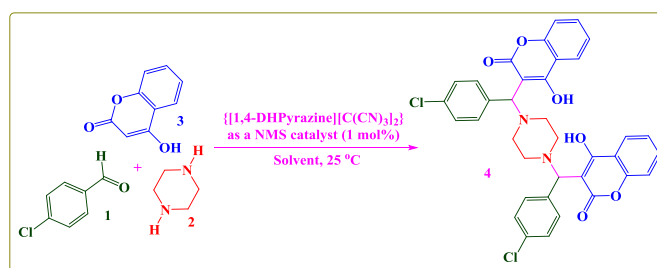
Table 3 Optimizing the amount of the catalyst and temperature in the reaction between 4-chlorobenzaldehyde, 4-hydroxycoumarin and piperazine using {[1,4-DHPyrazine][C(CN)₃]₂} as a NMS catalyst under solvent-free conditions

Entry	Catalyst loading (mol%)	Temperature (°C)	Time (min)	Yield ^a (%)
1	Catalyst-free	25	60	–
2	Catalyst-free	50	60	–
3	Catalyst-free	100	60	–
4	0.5	25	60	65
5	0.5	50	60	65
6	0.5	100	60	58
7	1	25	5	96
8	1	50	5	96
9	1	100	5	91
10	2	25	5	96
11	2	50	5	96
12	2	100	5	90

Reaction condition: 4-Chlorobenzaldehyde (1 mmol; 0.140 g), 4-hydroxycoumarin (1 mmol; 0.162 g), piperazine (1 mmol; 0.086 g)

^aIsolated yield

Table 4 Optimization of the reaction medium in the reaction between 4-chlorobenzaldehyde, 4-hydroxycoumarin and piperazine at room temperature using 1 mol % of {[1,4-DHPyrazine][C(CN)₃]₂} as a NMS catalyst



Entry	Solvent	Time (min)	Yield ^a (%)
1	Solvent-free	5	96
2	H ₂ O	10	95
3	C ₂ H ₅ OH	10	95
4	CH ₃ CN	15	95
5 ^b	CH ₂ Cl ₂	20	93
6	CH ₃ CO ₂ Et	20	93
7	<i>n</i> -Hexane	30	81
8	Toluene	30	85

Reaction condition: 4-Chlorobenzaldehyde (1 mmol; 0.140 g), 4-hydroxycoumarin (1 mmol; 0.162 g), piperazine (1 mmol; 0.086 g), {[1,4-DHPyrazine][C(CN)₃]₂} (1 mol%; 0.0026 g)

^aIsolated yield

^bReaction in CH₂Cl₂ as a solvent was investigated under reflux condition

all cases, the reaction proceeds readily to give the corresponding products in good to excellent yields (90–98%) in short reaction time. The results show that aldehydes with electron-donating substituents afford lower yields as compared to the ones with electron-withdrawing substituents. Also, hetero-aromatic aldehydes took longer time than aromatic aldehydes and provide lower yield of corresponding products.

A possible mechanism for the production of 3,3'-(piperazine-1,4-diylbis(arylmethylene))bis(4-hydroxy-2H-chromen-2-one) derivatives (4) has been proposed in Scheme 2. The mechanism of this reaction is similar to a Mannich-based pseudo-five-component reaction, actually a bidirectional three-component reaction of type ABBCC [49–52]. Firstly, {[1,4-DHPyrazine][C(CN)₃]₂} as a NMS catalyst activates the carbonyl group of the aromatic aldehyde (1) to provide intermediate (5). The nucleophilic attack of piperazine (2) to intermediate (5) was carried out to form the intermediate (6). Then, 4-hydroxycoumarin (3) perform nucleophilic attack to intermediate (6) and gives the 3,3'-(piperazine-1,4-diylbis(arylmethylene))bis(4-hydroxy-2H-chromen-2-one) derivatives (4) via the elimination of two water molecule and tautomerization.

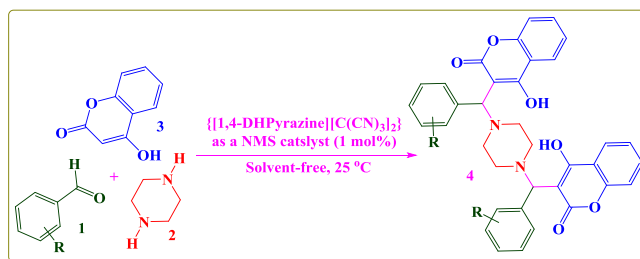
We further assessed the reusability of the NMS catalyst in the synthesis of 3,3'-(piperazine-1,4-diylbis(arylmethylene))bis(4-hydroxy-2H-chromen-2-one)s, because it is crucial to

approve that the highly active catalyst is recyclable [53]. We checked the reusability of the catalyst by scaling up to 10 mmol of each substrate using 10 mol% of NMS catalyst at room temperature under solvent-free condition. The selected model reaction between 4-chlorobenzaldehyde, 4-hydroxycoumarin and piperazine was repeated as far as yield didn't go lower than 90%. At the end of each repeated reaction, the catalyst is separated by filtration and then washed with ethyl acetate. As seen, from Fig. 9, the NMS catalyst can be reused up to six times without important loss of activity. The structure of reused NMS catalyst was also confirmed by FT-IR after its application in the reaction. Also, the size and morphology of reused catalyst was investigated by SEM and TEM analyses. These studies showed that the catalyst was recovered in nano size (Figs. S100–S102).

4 Conclusions

A novel nanostructured molten salt {[1,4-DHPyrazine][C(CN)₃]₂} (NMS) was produced. The molecular structure of NMSs was fully characterized by using various techniques including FT-IR, ¹H NMR, ¹³C NMR, mass, TGA, DTG, DTA, XRD, SEM and TEM analysis. The described NMSs was used as an efficient and

Table 5 Synthesis of 3,3'-(piperazine-1,4-diylbis(arylmethylene))bis(4-hydroxy-2*H*-chromen-2-one) derivatives in the presence of 1 mol% of {[1,4-DHPyrazine][C(CN)₃]₂} as a NMS catalyst under solvent-free conditions at room temperature



Entry	Product	M.p. (°C) (color)	Time (min)	Yield ^a (%)
4a		253–255 (White solid)	5	96
4b		244–246 (White solid)	10	93
4c		260–262 (White solid)	15	91

Table 5 (continued)

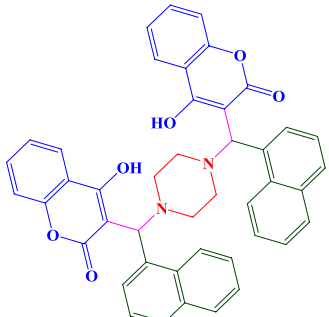
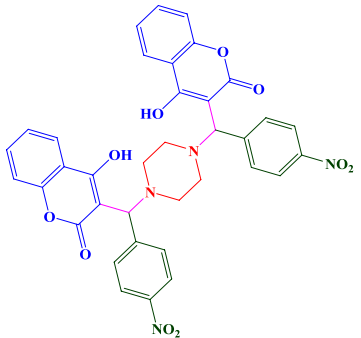
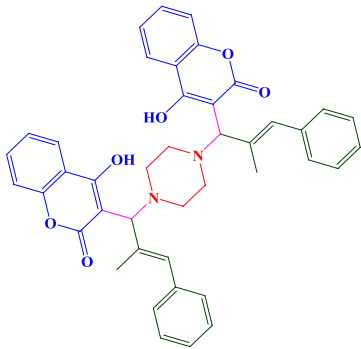
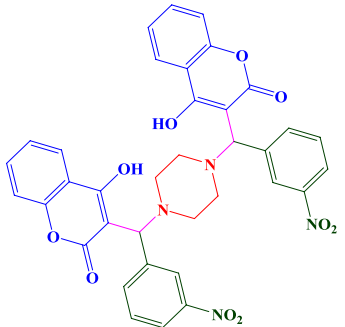
Entry	Product	M.p. (°C) (color)	Time (min)	Yield ^a (%)
4d		227–229 (Yellow solid)	10	96
4e		271–273 (Cream solid)	5	98
4f		203–205 (Cream solid)	15	91
4g		238–240 (Cream solid)	10	96

Table 5 (continued)

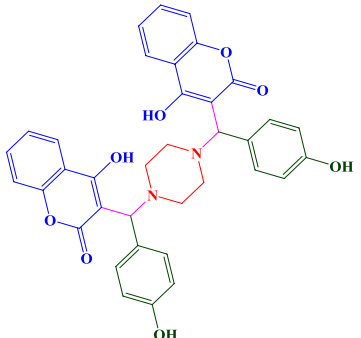
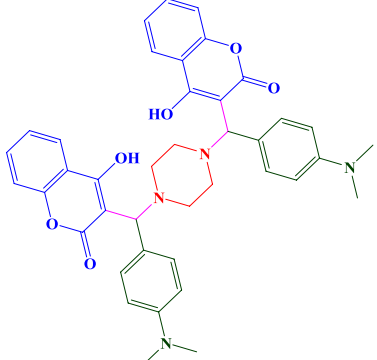
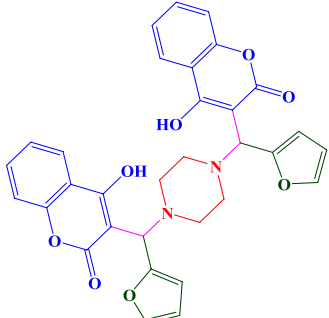
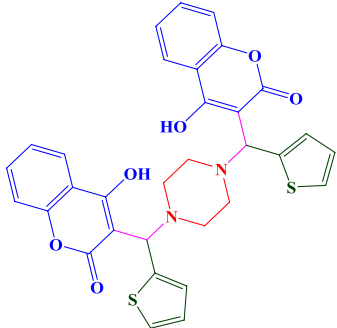
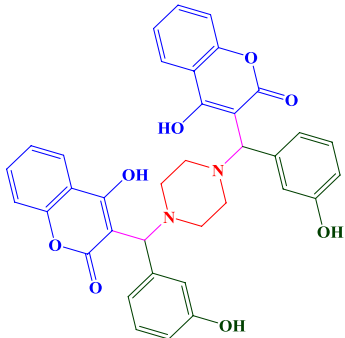
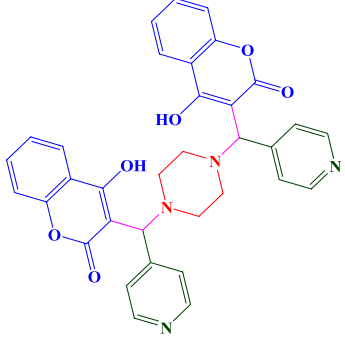
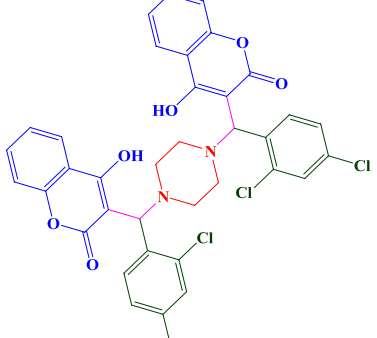
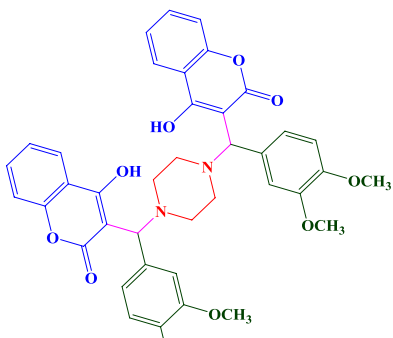
Entry	Product	M.p. (°C) (color)	Time (min)	Yield ^a (%)
4h		213–215 (Yellow solid)	15	92
4i		233–235 (Pink solid)	15	93
4j		324–326 (Brown solid)	20	90
4k		242–244 (Brown solid)	20	90

Table 5 (continued)

Entry	Product	M.p. (°C) (color)	Time (min)	Yield ^a (%)
4l		221–223 (Yellow solid)	20	90
4m		254–256 (Yellow solid)	20	90
4n		218–220 (Cream solid)	10	95
4o		269–271 (White solid)	10	93

Reaction condition: Aldehyde (1 mmol), 4-hydroxycoumarin (1 mmol; 0.162 g), piperazine (1 mmol; 0.086 g), {[1,4-DHPyrazine][C(CN)₃]₂} (1 mol%; 0.0026 g)

^aIsolated yield

Scheme 2 The probable mechanism for the synthesis of 3,3'-(piperazine-1,4-diylbis(arylmethylene))bis(4-hydroxy-2*H*-chromen-2-one) derivatives in the presence of {[1,4-DHPyrazine][C(CN)₃]₂} as a NMS catalyst

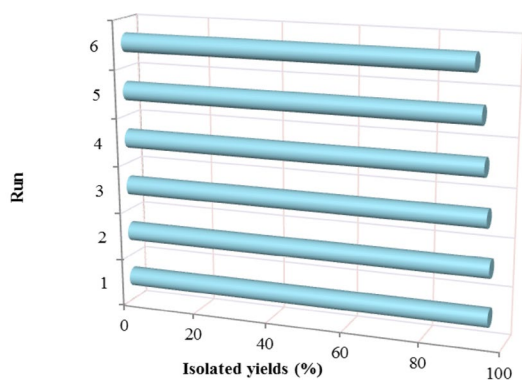
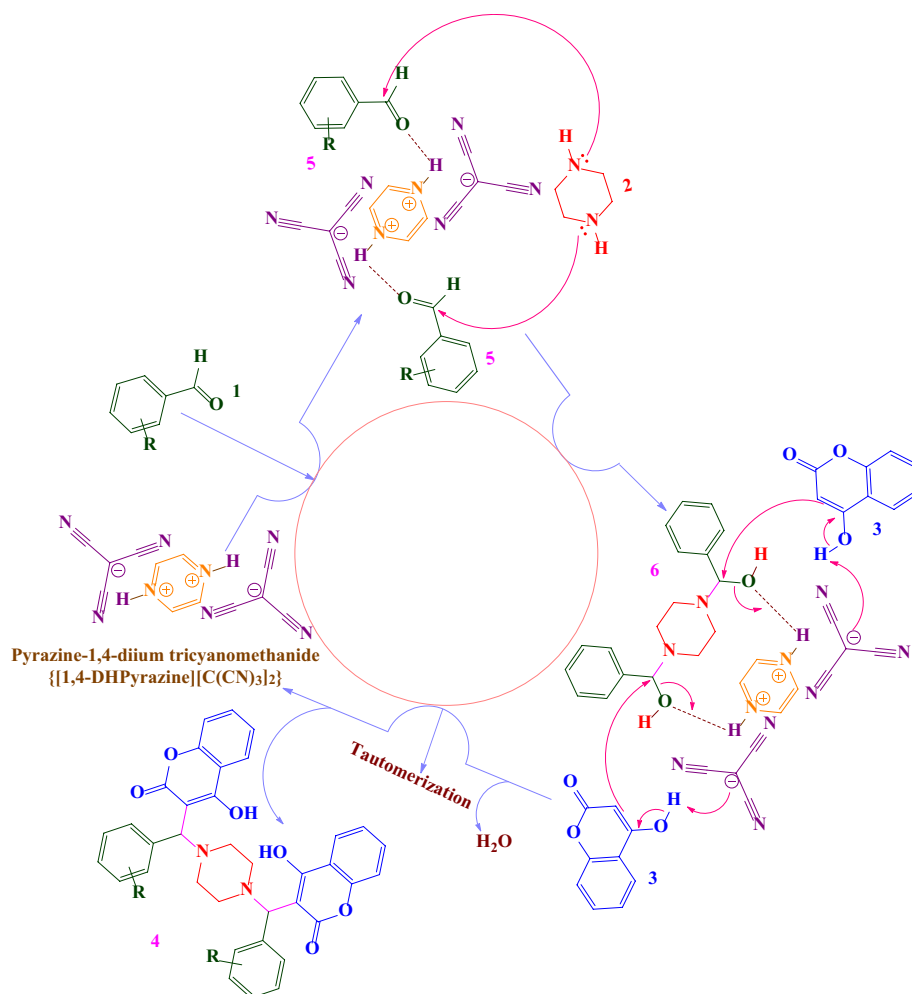


Fig. 9 Reusability studies of the {[1,4-DHPyrazine][C(CN)₃]₂} as a NMS catalyst on the synthesis of 3,3'-(piperazine-1,4-diylbis(arylmethylene))bis(4-hydroxy-2*H*-chromen-2-one) in 5 min

recyclable catalyst for the synthesis of novel 3,3'-(piperazine-1,4-diylbis(arylmethylene))bis(4-hydroxy-2*H*-chromen-2-one) derivatives. The NMS catalyst could be

reused for six consecutive cycles without loss of its activity. The combination of advantages showed by NMS catalyst, for example stability, reasonable catalytic activity and reusability, means that this catalyst may be investigated as a viable alternative in organic reactions in environmental and economic fields.

Acknowledgements We thank Bu-Ali Sina University and Iran National Science Foundation (INSF) for financial support (Grant of Allameh Tabataba'i's Award, Grant Number BN093), and National Elites Foundation to our research groups.

References

- Edlund C, Oh H, Nord CE (1999) Clin Microbiol Infect 1:51–53
- Chaudhary P, Kumar R, Verma AK, Singh D, Yadav V, Chhillar AK, Sharma GL, Chandra R (2006) Bioorg Med Chem 14:1819–1828
- Zhao HY, Prosser AR, Liotta DC, Wilson LJ (2015) Bioorg Med Chem Lett 25:4950–4955
- Kumar A, Gupta MK, Kumar M (2011) Tetrahedron Lett 52:4521–4525

5. Pallavi R, Saidulu K, Javed I, Srinivas O (2012) *Tetrahedron Lett* 53:5314–5317
6. Chhanda M, Sunil R, Ray J (2012) *Synth Commun* 42:3077–3088
7. Ghosh PP, Das AR (2012) *Tetrahedron Lett* 53:3140–3143
8. Hatnapure GD, Keche AP, Rodge AH, Birajdar SS, Tale RH, Kamble VM (2012) *Bioorg Med Chem Lett* 22:6385–6390
9. Beyeh NK, Valkonen A (2010) *Org Lett* 12:1392–1395
10. Long JZ, Jin X, Adibekian A, Li WW, Cravatt BF (2010) *J Med Chem* 53:1830–1842
11. Lee YB, Gong YD, Yoon H, Ahn CH, Jeon MK, Kong JY (2010) *Bioorg Med Chem* 18:7966–7974
12. Dou D, He G, Mandadapu SR, Aravapalli S, Kim Y, Chang KO, Groutas WC (2012) *Bioorg Med Chem Lett* 22:377–379
13. Patel RV, Kumari P, Rajani DP, Pannecouque C, De Clercq E, Chikhalia KH (2012) *Future Med Chem* 4:1053–1065
14. Patel RV, Kumari P, Rajani DP (2012) *J Enzyme Inhib Med Chem* 27:370–374
15. Xu J, Cao Y, Zhang J, Yu S, Zou Y, Chai X, Wu Q, Zhang D, Jiang Y, Sun Q (2011) *Eur J Med Chem* 46:3142–3148
16. Ibezim E, Duchowicz PR, Ortiz EV, Castro EA (2012) *Chemometr Intell Lab* 110:81–88
17. Johnson KE (2007) *Electrochem Soc Interface* 16:38–43
18. Adams DJ, McDonald IR (1974) *J Phys C Solid State Phys* 7:2761–2773
19. Wilkes JS, Mamantov G, Marassi R (1987) Vol 200. D Reidel Co, Dordrecht, p 217
20. Wasserscheid P, Keim W (2009) *Angew Chem Int Ed* 39:3772–3789
21. Taheri A, Lai B, Cheng C, Gu Y (2015) *Green Chem* 17:812–816
22. Taheri A, Liu C, Lai B, Cheng C, Pan X, Gu Y (2014) *Green Chem* 16:3715–3719
23. Taheri A, Pan X, Liu C, Gu Y (2014) *ChemSusChem* 7:2094–2100
24. García-Verdugo E, Altava B, Burguete MI, Lozano P, Luis SV (2015) *Green Chem* 17:2693–2713
25. Luska KL, Migowski P, Leitner W (2015) *Green Chem* 17:3195–3206
26. Zhu S, Wu Y, Chen Q, Yu Z, Wang C, Jin S, Ding Y, Wu G (2006) *Green Chem* 8:325–327
27. Van Rantwijk F, Lau RM, Sheldon RA (2003) *Trends Biotechnol* 21:131–138
28. Dupont J, Fonseca GS, Umpierre AP, Fichtner PFP, Teixeira SR (2002) *J Am Chem Soc* 124:4228–4229
29. Reichardt C (2007) *Org Process Res* 11:105–113
30. Sundermeyer W (1965) *Angew Chem Int Ed Engl* 4:222–238
31. Parvulescu VI, Hardacre C (2007) *Chem Rev* 107:2615–2665
32. Welton T (1999) *Chem Rev* 99:2071–2083
33. Lei Z, Dai C, Chen B (2014) *Chem Rev* 114:1289–1326
34. Hayes R, Gregory G, Warr GG, Atkin R (2015) *Chem Rev* 115:6357–6426
35. Amarasekara AS (2016) *Chem Rev* 116:6133–6183
36. Egorova KS, Ananikov VP (2014) *ChemSusChem* 7:336–360
37. Frade RFM, Afonso CAM (2010) *Hum Exp Toxicol* 29:1038–1054
38. Jastorff B, Störmann R, Ranke J, Mölter K, Stock F, Oberheitmann B, Hoffmann W, Hoffmann J, Nüchter M, Ondruschka B, Filser J (2003) *Green Chem* 5:136–142
39. Kianpour E, Azizian S, Yarie M, Zolfigol MA, Bayat M (2016) *Chem Eng J* 295:500–508
40. Zolfigol MA, Yarie M, Bagheri S (2016) *Synlett* 27:1418–1422
41. Zolfigol MA, Mansouri N, Bagheri S (2016) *Synlett* 27:1511–1515
42. Ghaderi H, Zolfigol MA, Bayat Y, Zarei M, Noroozizadeh E (2016) *Synlett* 27:2246–2250
43. Zolfigol MA, Khazaei A, Moosavi-Zare AR, Zare A, Kruger HG, Asgari Z, Khakyzadeh V, Kazem-Rostami M (2012) *J Org Chem* 77:3640–3645
44. Moosavi-Zare AR, Zolfigol MA, Zarei M, Noroozizadeh E, Beyzavi MH (2016) *RSC Adv* 6:89572–89577
45. Moosavi-Zare AR, Zolfigol MA, Noroozizadeh E (2016) *Synlett* 27:1682–1684
46. Zolfigol MA, Afsharnadery F, Bagheri S, Salehzadeh S, Maleki F (2015) *RSC Adv* 5:75555–75568
47. Zolfigol MA, Khazaei A, Alaie S, Bagheri S, Maleki F, Bayat Y, Asghari A (2016) *RSC Adv* 6:58667–58679
48. Zolfigol MA, Kiafar M, Yarie M, Taherpour A, Saeidirad M (2016) *RSC Adv* 6:50100–50111
49. Verkade JMM, Van Hemert LJC, Quaedflieg PJLM, Rutjes FPJT (2008) *Chem Soc Rev* 37:29–41
50. Hayashi Y, Urushima T, Shin M, Shoji M (2005) *Tetrahedron* 61:11393–11404
51. Zolfigol MA, Bahrami-Nejad N, Afsharnadery F, Bagheri S (2016) *J Mol Liq* 221:851–859
52. Safaiee M, Zolfigol MA, Bahrami-Nejad N, Afsharnadery F, Bagheri S (2015) *RSC Adv* 5:102340–102349
53. Yu B, Xie JN, Zhong CL, Li W, He LN (2015) *ACS Catal* 8:3940–3944